REPORT DOCUMENTATION PAGE

Form Approved
OMB No. 0704-0188

PLEASE DO NOT RETURN YOUR FORM TO THE ABOVE ORGANIZATION.

1. REPORT DATE *(DD-MM-YYYY)*	2. REPORT TYPE	3. DATES COVERED *(From - To)*
20-02-2012	Conference Proceedings	

4. TITLE AND SUBTITLE
Iron Drinking Water Pipe Corrosion Products: Concentrators of Toxic Metals

5a. CONTRACT NUMBER

5b. GRANT NUMBER

5c. PROGRAM ELEMENT NUMBER
0601153N

6. AUTHOR(S)
Tammie L. Gerke, Todd P. Luxton, J. Barry Maynard and Brenda J. Little

5d. PROJECT NUMBER

5e. TASK NUMBER

5f. WORK UNIT NUMBER
73-9576-02-5

7. PERFORMING ORGANIZATION NAME(S) AND ADDRESS(ES)
Naval Research Laboratory
Oceanography Division
Stennis Space Center, MS 39529-5004

8. PERFORMING ORGANIZATION REPORT NUMBER
NRL/PP/7303--12-1548

9. SPONSORING/MONITORING AGENCY NAME(S) AND ADDRESS(ES)
Office of Naval Research
One Liberty Center
875 North Randolph Street, Suite 1425
Arlington, VA 22203-1995

10. SPONSOR/MONITOR'S ACRONYM(S)
ONR

11. SPONSOR/MONITOR'S REPORT NUMBER(S)

12. DISTRIBUTION/AVAILABILITY STATEMENT
Approved for public release, distribution is unlimited.

13. SUPPLEMENTARY NOTES

14. ABSTRACT
The capability of iron pipe corrosion products in active drinking water systems to concentrate metal ions, such as Pb, Sr and V from treated drinking water and mechanisms that can cause consumer exposures and releases back into the environment will be presented. We propose that sorption is the main mechanism concentrating metal ions on the surfaces of iron corrosion products. Typically metal concentrations in the corrosion products are an order(s) of magnitude greater than in the water entering the distribution system. Several mechanisms, including hydraulic disturbances, chemical disassociations, road work, or earthquakes, can result in acute exposures of consumers or concentrated releases of toxic metal back into the environment.

15. SUBJECT TERMS
strontium, lead, vanadium, XANES, drinking water pipes, corrosion products

16. SECURITY CLASSIFICATION OF:			17. LIMITATION OF ABSTRACT	18. NUMBER OF PAGES	19a. NAME OF RESPONSIBLE PERSON
a. REPORT	b. ABSTRACT	c. THIS PAGE			Brenda Little
Unclassified	Unclassified	Unclassified	UU	12	19b. TELEPHONE NUMBER *(Include area code)* (228) 688-5494

Paper No.
2637

Iron Drinking Water Pipe Corrosion Products: Concentrators of Toxic Metals

Tammie L. Gerke and J. Barry Maynard
Department of Geology
University of Cincinnati
Cincinnati, OH, 45221-0013
USA

Todd P. Luxton and Kirk G. Scheckel
U.S. Environmental Protection Agency, ORD,
NRMRL, LRPCD
26 West Martin Luther King Dr.
Cincinnati, OH, 45268
USA

Brenda J. Little
Naval Research Laboratory
Stennis Space Center, MS 39525
USA

ABSTRACT

The capability of iron pipe corrosion products in active drinking water systems to concentrate metal ions, such as Pb, Sr and V from treated drinking water and mechanisms that can cause consumer exposures and releases back into the environment will be presented. We propose that sorption is the main mechanism concentrating metal ions on the surfaces of iron corrosion products. Typically metal concentrations in the corrosion products are an order(s) of magnitude greater than in the water entering the distribution system. Several mechanisms, including hydraulic disturbances, chemical disassociations, road work, or earthquakes, can result in acute exposures of consumers or concentrated releases of toxic metals back into the environment.

Key words: strontium, lead, vanadium, XANES, drinking water pipes, corrosion products

INTRODUCTION

As the world's population increases, so will the demand for safe drinking water,[1] which is essential for human existence. Thus, developing an understanding now of how metals concentrate to, and later desorb from, corroded lead and iron drinking water pipes is critical to being able to deliver safe drinking water to consumers worldwide.

Lead (Pb) drinking water pipes and associated corrosion products are a known health risk. In addition Pb corrosion products may be sinks for other metals such as chromium (Cr), copper (Cu), manganese (Mn), and zinc (Zn). These metals are toxic when ingested from drinking water and accordingly are

regulated by the United States Environmental Protection Agency (USEPA).[2] Lead piping constitutes a small portion of a drinking water distribution system infrastructure.

Iron (Fe) pipes typically constitute the majority of distribution system's infrastructures and recent studies indicate that Cr, Co, Mn, Pb, and Zn concentrate on the corroded inner surfaces of the pipes.[3-6] The USEPA reviews its drinking water standards periodically as new research determines additional metals that may be toxic if ingested.

Ingestion of vanadium (V) and non-radioactive strontium from drinking water (Sr) has recently been suggested to be a threat to human health[7-11]. Based on these findings, the USEPA listed V on the Drinking Water Contaminant Candidate List 2 (CCL 2) and V and Sr^{2+} on the CCL 3[12] which, if approved, would result in regulatory drinking water limits for both.

In May of 2012 the Director of the USEPA signed the Unregulated Contaminant Monitoring Rule 3 which includes V and Sr^{2+} (UCMR3)[13]. Sampling locations are at the point-of-entry into and at the point-of-maximum residence time in a drinking water distribution system (DWDS). These locations were chosen because water chemistry and quality are changeable as drinking water travels through and interacts with the DWDS infrastructure and associated corrosion products.[13, 14] Reporting to the USEPA is required if the Sr^{2+} water concentration exceeds 0.3 $\mu g\ L^{-1}$ or V water concentration exceeds 0.2 $\mu g\ L^{-1}$ at either location in the DWDS. Average V drinking water concentrations are not available. Crans et al.[15] reported that typical V concentrations in surface and ground water were approximately 40 $mg\ L^{-1}$. The highest reported concentrations in surface water range from 160 to 220 $mg\ L^{-1}$, and are associated with volcanic regions.[16] Average Sr^{2+} concentration in United States drinking water is approximately 1.1 $mg\ L^{-1}$.[10] Therefore, it is likely that the drinking water of numerous DWDS will exceed the reporting limits for V and Sr^{2+}.

The potential for Sr, V and other toxic metals to concentrate in lead and iron corrosion products is not well documented. Neither is the potential for release if corrosion products are disturbed, either hydraulically or chemically, creating pulses of elevated metal concentrations in the water or metal-rich particulates that could reach the consumer tap.[4, 17]

The objective of the current study was to determine the abundance, distribution and bonding mechanisms of V and Sr^{2+} in surface layers of iron corrosion products from lead, unlined cast iron and galvanized iron drinking water pipes. In addition to traditional physiochemical characterization techniques we examined V and Sr^{2+} and other metals distribution using micro X-ray fluorescence mapping (μ-XRF). Binding mechanisms of V and Sr^{2+} within the corrosion products was examined using *in-situ* micro X-ray adsorption near edge spectroscopy (μ-XANES). The amount of V and Sr^{2+} that could potentially be reintroduced into drinking water from iron corrosion products was examined using particulates collected at the point-of-entry into a consumer's home. The combined data provide a preliminary assessment of the extent of a potential reservoir of V and Sr^{2+} in a single drinking water distribution system and its mobility.

EXPERIMENTAL PROCEDURE

Sample selection and preparation

All pipe sections were cut longitudinally with a saw, allowed to air dry for up to 72 h, and imaged using a Canon G3† digital camera. A Pb service line and two galvanized Fe premise pipes were obtained from Utility B (UB), a fully operational drinking water distribution system (DWDS). Mound-shaped Fe

† Trade name.

corrosion products were obtained from an unlined cast iron residential main from Utility A (UA) also a fully operational DWDS. While in service, all pipes were exposed to daily periods of stagnation.

Sub-samples (up to 3.0 g) from iron pipes were obtained from regions within the mounds, i.e., core, shell and surface layers[18] (Figure 1). Colors for each layer were determined using standard color chart of Cornell and Schwertmann.[19] Lead corrosion product sub-samples were obtained based on color.

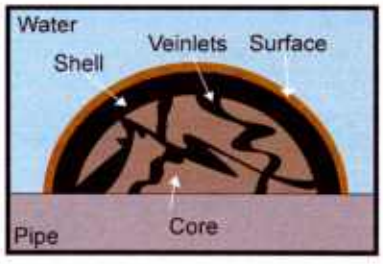

Figure 1: Schematic of idealized internal structure of a mound-shaped iron corrosion product from DWDS (after)[20-22]

All corrosion product samples were ground by hand with an agate mortar and pestle and aliquots were used for mineralogical and chemical analyses. Aliquots of each Pb sample were analyzed by ICP-OES at the United States Geologic Survey, Denver, Colorado USA. Subsamples from each region of the Fe corrosion products (approximately 0.25 g) were mixed with 2.25 g of cellulose and pressed into 31 mm pellets for X-ray fluorescence (XRF) analysis.

Two representative Fe corrosion products from UA (samples UA11 and UA13) and one from UB were processed for synchrotron analyses following protocols of Gerke et al., 2010 and 2012. Each section was digitally photographed. These images were used in selecting locations to obtain μ-XRF elemental maps and for in-situ μ-XANES analyses.

Sediment filter collection and preparation

A 25 cm long sediment filter in use for four years (2008 to 2012) in UA was removed from a home, transported to the laboratory and air-dried. The filter was cut in half longitudinally and laterally (Figure 2) and two 12.5 cm long strips were removed from the outer wall. These strips were placed in sterile beakers and heated to 200 °C for 1 h. Heating melted the filter material, creating disks that were used for XRF analysis (Figure 1). The heating did not alter the concentrations of the metals of interest.

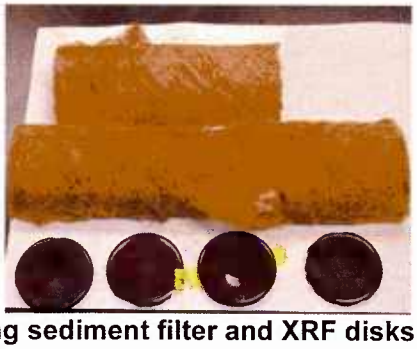

Figure 2: Image of a 25 cm long sediment filter and XRF disks from a home in Utility A. Filter was in use for four years.

Powder X-ray diffraction (XRD)

Powder XRD analyses for all Pb samples were conducted using a Scintag† XDS-2000 with Cu Kα radiation at USEPA, Cincinnati, OH (Gerke et al. 2009). All Fe samples were analyzed using a Siemens D-500 automated diffractometer system equipped with a Cu Kα tube at the Department of Geology, University of Cincinnati, Cincinnati, OH. Crystalline phases were identified following the protocol of Gerke et al.[4].

ICP-OES and X-ray fluorescence analyses

Scale material from layers of the Pb pipe corrosion products were analyzed by ICP-OES at the US Geological Survey in Denver. Pressed pellets and sediment filter disks were analyzed for major oxides and trace elements using a Rigaku† 3070 X-ray fluorescence spectrometer (Department of Geology, University of Cincinnati, Cincinnati, OH). Intensity data were converted to percent (by weight) or mg kg^{-1} following the protocol of Gerke et al.[4].

Synchrotron μ-X-ray absorption near edge structure (μ-XANES) and μ-XRF mapping run conditions and analysis

X-ray μ-beam studies were performed at beamline XOR/PNC 20 BM-B[23] and MRCAT Sector 10[24] of the Advanced Photon Source (APS), Argonne National Laboratory (Argonne, IL). The protocols for micro-XANES and micro-XRF mapping for V and Pb are published in Gerke et al.[3,4]. Three Sr *K*-edge μ-XANES scans were collected at ambient temperature in fluorescence mode with a solid-state 13-element germanium solid-state Canaberra† detector for samples UA11 and UA13 at beamline XOR/PNC 20 BM-B. The monochromator beam energy position at both beamlines was calibrated by assigning the first inflection of the adsorption edge of Sr^{2+} to 1,605 eV following the protocol of O'Day et al.[25] Bulk XANES scans of the Pb, V and Sr standards were collected. All spectra were placed on the same energy grid by element and aligned, averaged, normalized, and the background removed by spline fitting using IFEFFIT.[26]

Linear combination fitting (LCF) was conducted on the first derivative of the normalized (E) XANES spectra of the standards and samples. Levenberg–Marquardt least squares algorithm was applied to a fit range of -10 or −20 to 80 eV. Each LCF analysis encompassed 124 to 180 data points of a given sample spectrum and five standard spectra. Best-fit scenarios were defined as having the smallest residual error and the sum of all fractions was close to 1. To fully describe any particular sample within 1% reproducible error, a minimum of two components was necessary, and results have a ±10 percent accuracy.

RESULTS AND DISCUSSION

Strontium in the Fe pipe and sediment filter particulate from Utility A

Strontium concentrations in the surface layers of the 18 iron corrosion products from UA ranged from 3 to 128 mg kg^{-1} (sample UA11 and UA13 data provided; Table 1). The average Sr^{2+} concentration for surface layers was 38 mg kg^{-1} and the Sr^{2+} concentrations of the sediment filter particulates ranged from 39.74 to 40.77 mg kg^{-1}, with an average of 40.26 mg kg^{-1} (Table 1).

† Trade name.

† Trade name.

Table 1. Bulk powder X-ray fluorescence results for Fe corrosion products from four drinking water distribution systems and two iron particulate sediment filter samples.

Utility	Region	Metals							
		Fe	Mn	Cr	Cu	Pb	Sr	V	Zn
		%				mg kg^{-1}			
Iron pipe samples									
UA11	Surface	45.1	0.15	40	59	8	76	58	32
	Shell	45.5	0.11	23	12	9	7	*bd*	11
	Veinlets	54.7	0.05	46	5	11	10	5	8
	Core	57.9	0.04	43	11	9	65	*bd*	10
UA13	Surface	34.1	0.28	44	47	24	128	83	39
	Shell	54.6	0.10	29	6	3	28	17	7
	Veinlets	55.7	0.03	13	15	9	12	*bd*	4
	Core	55.6	0.03	9	4	11	10	*bd*	3
UBFe1	Surface	41.2	10.45	80	19797	69981	22	899	3866
	Shell	98.6	0.73	*bd*	35	5356	2	56	762
	Core	89.5	1.43	22	64	12418	7	230	1860
Sediment filter particulate samples									
UASFLT1		8.71	0.24	23	6522	45100	40	12	1692
UASFLT2		9.40	0.21	7	4692	49155	41	13	1365
Lead pipe samples									
UBPb1	L1	4.9	2.7	47	11000	406100	139	5480	770
UBPb1	L2	0.82	0.49	30	3670	502100	228	2650	400
UBPb1	L3	0.08	0.04	12	1020	679400	90	716	114
UBPb2	-	-	-	-	-	-	-	-	-
UBPb2	L2	2.3	2.00	129	11000	522000	88	8500	260
UBPb2	L3	0.36	0.27	49	3860	629000	104	2750	744

bd = below detection

In-situ μ-XANES spectra from samples UA11 (one spectrum) and UA13 (two spectra) are shown in Figure 3. The Sr *K*-edge in-situ μ-XANES spectra for UA11 Point 1 and UA13 Points 1 and 2 have prominent peaks at 16,110, 16,120, and 16,156 eV (Figure 3). The energies of the predominant sample peaks corresponded to characteristic peaks of the standards (Table 2).

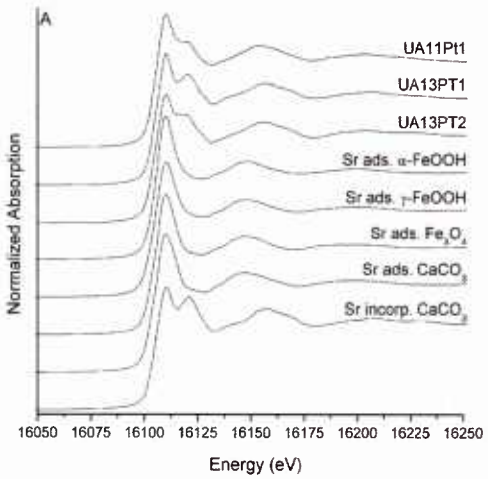

Figure 3: Strontium *K*-edge spectra for bulk XANES Sr standards and the in-situ μ-XANES for samples a) UA11 point 1 (UA11PT1) and UA13 points 1 and 2 (UA13PT1, and UA13PT2). Sr standards are $CaCO_3$ in which some of the Ca^{2+} sites have been filled with Sr^{2+} (Sr incorp. $CaCO_3$) and Sr adsorbed to the following: α-FeOOH (Sr abs. α-FeOOH), γ-FeOOH (Sr abs. γ-FeOOH), Fe_3O_4 (Sr abs. Fe_3O_4), and $CaCO_3$ (Sr abs. $CaCO_3$).

Table 2. Strontium *K*-edge μ-XANES characteristic peak energies for the five Sr standards.

Standard	Characteristic Peaks (eV)			
	16,110.6	16,120	16,148	16,156.2
Sr abs. α-FeOOH	X		X	
Sr abs. γ-FeOOH	X		X	
Sr abs. Fe_3O_4	X		X	
Sr abs. $CaCO_3$	X		X	
Sr incorp. $CaCO_3$	X	X		X

LCF spectra, generated using all standards and the μ-XANES spectrum of a given sample, were superimposed on the first derivative spectrum of UA11 and UA13 (Figure 4). Sixty to 83.8% of the Sr^{2+} was adsorbed to or bound in $CaCO_3$ (Table 3). This finding was not unexpected because Sr^{2+} has a high affinity for binding with or adsorbing to $CaCO_3$. [27-30] The remaining Sr^{2+} in the surface layers was adsorbed to α-FeOOH (16 to 39%) (Table 3). Based on the work of Carroll et al.[31] and Sahai et al.[32] Sr^{2+} was likely adsorbed to α-FeOOH by outer-sphere complexation.

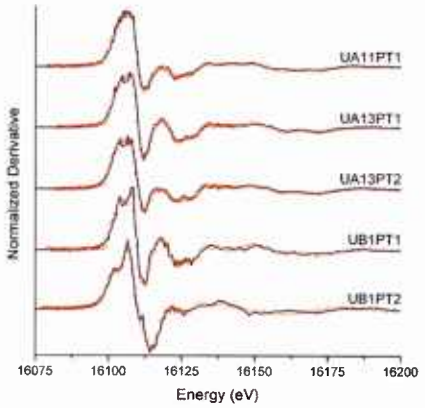

Figure 4: a) Linear combination fitting (red lines) and the first derivative of the normalized mu(E) (black lines) of the μ-XANES of Sr *K*-edge spectra for UA11PT1, UA13PT1, UA13PT2, and UB1PT1.

Table 3. Linear combination fitting results for Sr *K*-edge μ-XANES spectra in Fig. 4. Data presented as weighted percents (±10%) over the fit range of -20 to 80 eV.

Sample ID	Sr abs. α-FeOOH %	Sr abs. γ-FeOOH %	Sr abs. $CaCO_3$ %	Sr incorp. $CaCO_3$ %	R-factor
Chlorine Disinfection					
UA11 Point 1	39.1	-	-	60.9	0.0196
UA13 Point 1	16.2	-	-	83.8	0.0235
UA13 Point 2	25.3	-	-	74.7	0.0004

Vanadium in the Pb and Fe pipes from Utility B

Vanadium concentrations in the surface layers of the 14 lead corrosion products from UB ranged from 237 to 8,500 mg kg^{-1}. The average V concentration for surface layers was 3,260 mg kg^{-1}. Vanadium concentrations in the surface layers of three iron pipes from UB ranged from 9 to 86 mg kg^{-1}, with an average of 39 mg kg^{-1}. Data for two representative Pb corrosion samples (UBPb1 and UBPb2) and one representative Fe corrosion product (UBFe1) are provided in Table 1.

Micro-XRF mapping of samples UBPb2 and UBFe1 found regions of discrete high vanadium concentration in the outer most portions of the corrosion products (Figure 5; only UBFe1 presented).

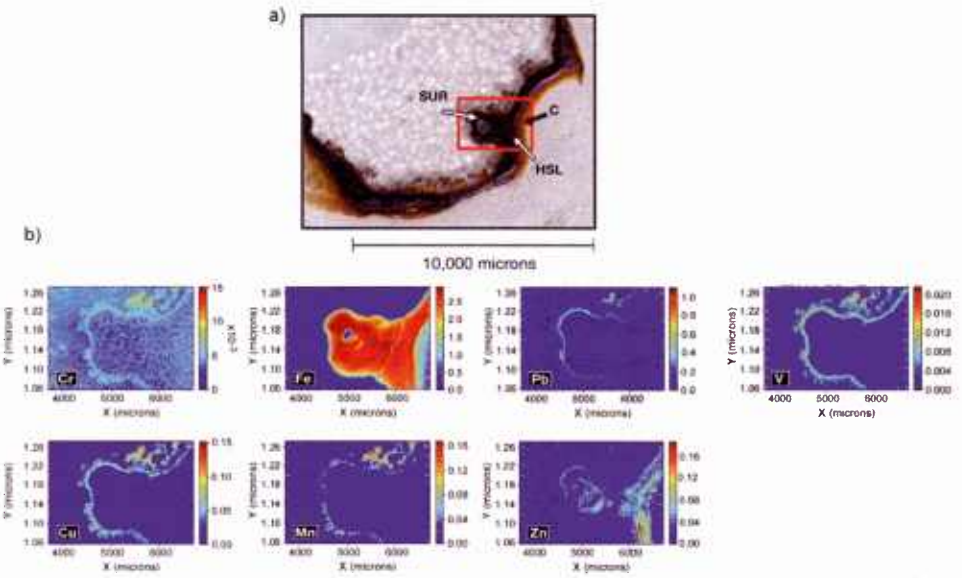

Figure 5: a) is a digital image of the 35 micron thick cross-section of UBFe1. The red box corresponds to the general region mapped by μ-XRF and the arrows indicate the core (C), shell layer (HSL), and surface layer and b) is the μ-XRF maps of the distribution and relative concentration of Cr, Cu, Fe, Mn, Pb, V, and Zn. Where blue indicates the lowest relative concentrations and red the highest relative concentrations.

Locations of relatively high V concentrations in UBPb2 and UBFe1 were analyzed by μ-XANES. The μ-XANES spectra had distinct normalized pre-edge peak positions between 5,469.46 and 5,469.5 eV with an absolution position approximately 4.5 eV above 5,465 eV (absolution position for V metal). Also intensities ranged from 0.928 to 1.046 and the absolute derivative peak positions of the main edge were between 16.44 and 16.52 eV. Robust methods developed by Chaurand[33] and Wong et al.[34] were used in this study to identify the V-rich phases. Vanadinite [$Pb_5(V^{5+}O_4)_3Cl$] was the vanadium-rich phase identified based on the normalized pre-edge peak positions (Figure 6)(Table 4).[33, 34]

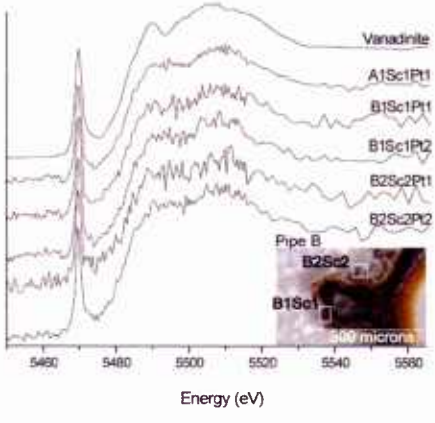

Figure 6: Normalized μ-XANES of V *K* edge spectra from SampleB1. White boxes in the digital images are the locations of the μ-XRF maps for pipe B. The notation for the sample IDs is as follows: B1 refers to the pipe, Sc1 or Sc2 refers to the μ-XRF map number for a given sample, and Pt1 or Pt2 refers to the location within a given μ-XRF that the V *K*-edge spectra were obtained.

Table 4. Detailed XANES analysis for intensity and position of pre-edge peak and derivative main edge peak position.

Sample Identification	Normalized Intensity	Absolution Position (eV)	Main Edge $E_{1/2}$ (eV)
Samples			
UBFe1 (Sc1Pt1)	1.011	4.48	16.45
UBFe1 (Sc1Pt2)	0.998	4.48	16.45
UBFe1 (Sc2Pt1)	1.000	4.49	16.49
UBFe1 (Sc2Pt2)	1.051	4.49	16.49
UPb2 (Pt2)	1.010	4.47	16.49
References			
Vanadinite	0.996	4.50	16.49
Lenoblite	0.398	5.20	17.05
V(V) Oxide	0.320	5.62	15.30
V(IV,V) Oxide	0.381	4.71	14.71
V metal	0.281	0.98	8.80

Ninety-one to 98% of the V present in these samples was present as vanadinite and the remaining 2 to 9% percent was identified as V(V) oxide, based on LCF data (Table 5). The presence of V(V) oxide could suggest that the vanadate oxyanion is forming or that vanadate ions are adsorbing to available Pb ions or onto the iron oxide/oxyhydroxide mineral surfaces within the iron pipe corrosion by-products.

Table 5. Linear combination fitting results for vanadium XANES spectra in Figure 5. Data presented as weighted percents over a fit range of -20 to 80 eV.

Sample	References					
	Vanadinite	Lenoblite	V(V) Oxide	V(IV,V) Oxide	V metal	R-factor [a]
UBFe1 (Sc1Pt1)	91.0		9.0			0.019
UBFe1 (Sc1Pt2)	94.2		5.8			0.016
UBFe1 (Sc2Pt1)	95.3		4.7			0.015
UBFe1 (Sc2Pt2)	97.7		2.3			0.012
UBPb2 (Pt2)	95.2		4.8			0.002

The notation for the sample IDs is as follows: B1 refers to the pipe, Sc1 or Sc2 refers to the μ-XRF map number for the given sample, and Pt1 or Pt 2 refers to the location within a given μ-XRF map where the V *K-edge* spectra were obtained. [a] R-factor = $[(\text{data-fit})^2]/[\text{data}^2]$

Distribution of other toxic metals in Pb and Fe pipe corrosion products

Bulk XRF analyses of Pb and Fe pipe corrosion products, regardless of drinking water distribution system, show that in general the highest concentrations of Cr, Cu, Fe, Mn, Ni, Pb, Sr, V, and Zn tended to be in the surface layers (Table 1). The fine-scale distribution of these elements mapped using synchrotron-based μ-XRF (Figure 5) displayed similar trends.

CONCLUSIONS

Strontium concentrations in the Fe corrosion products from UA ranged from 3 to 128 mg kg^{-1} and the Sr^{2+} concentration in the associated drinking water was 300 $\mu g\ L^{-1}$. For UB the Pb and Fe corrosion product Sr^{2+} concentrations ranged from 22 to 139 mg kg^{-1} and the Sr^{2+} concentration in the treated drinking water ranged from 164 to 174 $\mu g\ L^{-1}$.

In Case of V, from UB the Pb corrosion products had concentrations that ranged from 5,480 to 8,500 mg kg^{-1} (Pb corrosion) and in the Fe corrosion products the concentration was 899 mg kg^{-1} (Table 1). The associated V drinking water concentration for UB was 1.4 to 1.7 $\mu g\ L^{-1}$. Vanadium concentrations in the Fe corrosion products from UA ranged from 58 to 83 mg kg^{-1} and the V concentration in the associated drinking water was below detection (1.0 $\mu g\ L^{-1}$).

Average V and Sr^{2+} concentration in the filter particulates from UA were 12 mg kg-1 and 40 mg kg^{-1}, respectively. These concentrations were approximately the same as those of the surface layers of the Fe corrosion products examined from UA (Table 1). Also the concentrations of Cr, Cu, Fe, Mn, Pb, and Zn were similar to the concentrations found in surface layers of Pb corrosion products of that same DWDS (data not shown) and UB (Table 1). Regardless of the distribution system, it is clear that Pb and Fe corrosion products not only concentrate toxic metals but in concentrations that are at least an order of magnitude greater than the concentration found in the water to which they were exposed. These findings indicate the potential of large toxic metal reservoirs in distribution systems that, if disturbed, could produce pulses of drinking water with elevated toxic metal concentrations.

ACKNOWLEDGEMENTS

PNC/XOR facilities at the Advanced Photon Source, and research at these facilities, are supported by the U.S. Department of Energy - Basic Energy Sciences, a major facilities access grant from NSERC, the University of Washington, Simon Fraser University and the Advanced Photon Source. Use of the Advanced Photon Source is also supported by the U.S. Department of Energy, Office of Science, Office of Basic Energy Sciences, under Contract DE-AC02-06CH11357. MRCAT operations are supported by the Department of Energy and the MRCAT member institutions. This research has not been subject to Agency review and, therefore, does not necessarily reflect the views of the Agency. Mention of trade names of commercial products and companies does not constitute endorsement or recommendation for use. All ICP analyses were conducted by the United States Geological Survey's Mineral Resource Surveys Program under Interagency Agreement DWI4999901 under the direction of Dr. Stephen A. Wilson. We thank M. K. DeSantis and J. Dorch for photographs of the iron corrosion products and Mathew Jones for some sample preparation and Dr. R. B. Wanty, US Geological Survey. We also thank Dr. S. Held for use of his personal macros used in portions of the data processing, and Dr. R. Gordon for providing some standard material for the V *K*-edge m-XANES analysis. Dr. Little was funded by the Linda Chrisey, Office of Naval Research. NRL publication NRL/PP/7303—12-1548.

REFERENCES

1. NRC: 'Water Reuse: Expanding the Nation's Water Supply Through Reuse of Municipal Wastewater', 2012, Washington, DC, National Academy Press.
2. USEPA: 'National Primary Drinking Water Regulations', 2009.
3. T. L. Gerke, K. G. Scheckel, and M. R. Schock: 'Identification and Distribution of Vanadinite ($Pb_5(V^{5+}O_4)_3Cl$) in Lead Corrosion By-Products', *Environmental Science & Technology*, 43, 12 (2009): p. 4412.
4. T. L. Gerke, K. G. Scheckel, and J. B. Maynard: 'Speciation and Distribution of Vanadium in Drinking Water Iron Pipe Corrosion By-products', *Science of the Total Environment*, 408, (2010): p. 5848.

5. C. Y. Peng and G. V. Korshin: 'Speciation of trace inorganic contaminants in corrosion scales and deposits formed in drinking water distribution systems', *Water research*, 45, 17 (2011): p. 5553.
6. C. Y. Peng, G. V. Korshin, R. L. Valentine, A. S. Hill, M. J. Friedman, and S. H. Reiber: 'Characterization of elemental and structural composition of corrosion scales and deposits formed in drinking water distribution systems', *Water research*, 44, 15 (2010): p. 4570.
7. J. Eikenberga, A. Triccab, G. Vezzua, P. Stilleb, S. Bajoa, and M. Ruethi: '$^{228}Ra/^{226}Ra/^{224}Ra$ and $^{87}Sr/^{86}Sr$ isotope relationships for determining interactions between ground and river water in the upper Rhine valley', *Journal of Environmental Radioactivity*, 54, (2001): p. 133.
8. S. Langley, A. G. Gault, A. Ibrahim, Y. Takahashi, R. Renaud, D. Fortin, I. D. Clark, and F. G. Ferris: 'Sorption of strontium onto bacteriogenic iron oxides', *Environmental Science and Technology*, 43, 4 (2009): p. 1008.
9. S. P. Nielsen: 'The biological role of strontium', *Bone*, 35, (2004): p. 583.
10. P. Watts and P. Howe: 'Strontium and Strontium Compounds', *Concise International Chemical Assessement* 77 (2010): p. 63.
11. ATSDR: 'Toxicological profile for Vanadium', (ed. P. H. S. Agency for Toxic Substances and Disease Registry (Draft for Public Comment)), 2009, Atlanta, GA, U.S. Department of Health and Human Services.
12. USEPA: 'Drinking Water Conntamination Candidate List 3 Final Notice', 51850-51862; 2009.
13. USEPA: 'Unregulated Contaminant Monitoring Rule 3 (UCMR 3)', 26071-26101; 2012.
14. A. O. Al-Jasser: 'Chlorine decay in drinking-water transmission and distribution systems: pipe service age effect', *Water research*, 41, 2 (2007): p. 387.
15. D. C. Crans, S. S. Amin, and A. D. Keramidas: 'Chemistry of Relevance to Vanadium in the Environment', in 'Vanadium in the Environment', (ed. J. O. Nriagu), 73-95; 1998, New York, John Wiley & Sons, Inc.
16. E. Veschetti, D. Maresca, L. Lucentini, E. Ferretti, G. Citti, and M. Ottaviani: 'Monitoring of V(IV) and V(V) in Etnean drinking-water distribution systems by solid phase extraction and electrothermal atomic absorption spectrometry', *Microchemical Journal*, 85, 1 (2007): p. 80.
17. S. Triantafyllidou, J. Parks, and M. Edwards: 'Lead Particles in Potable Water', *Journal of the American Water Works Association*, 99, 6 (2007).
18. P. Sarin, V. L. Snoeyink, J. Bebee, K. K. Jim, M. A. Beckett, W. M. Kriven, and J. A. Clement: 'Iron release from corroded iron pipes in drinking water distribution systems: effect of dissolved oxygen', *Water research*, 38, 5 (2004): p. 1259.
19. R. M. Cornell and U. Schwertmann, *The Iron Oxides; Structure, Properties, Reactions, Occurrences and Uses*, (Darmstadt, Wiley-VCH Verlag GmbH & Co. KGaAl, 2003), p. 664.
20. J. R. Baylis: 'Prevention of Corrosion and Red Water', *Journal of the American Water Works Association*, 15, (1926).
21. P. Sarin, V. L. Snoeyink, D. A. Lytle, and W. M. Kriven: 'Iron Corrosion Scales: Model for Scale Growth, Iron Release and Colored Water Formation', *Journal of Environmental Engineering*, 130, (2004).
22. T. L. Gerke, J. B. Maynard, M. R. Schock, and D. A. Lytle: 'Physio-chemical Characterization of Five Iron Tubercles from a Single Drkinking Water Distribution System: Possible New Insights on Their Formation and Growth', *Corros. Sci.*, 50, (2008).
23. S. M. Heald, D. L. Brewe, E. A. Stern, K. H. Kim, F. C. Brown, D. T. Jiang, E. D. Crozier, and R. A. Gordon: 'XAFS and micro-XAFS at the PNC-CAT beamlines.', *Journal of Synchrotron Radiation*, 6, (1999): p. 347.
24. C. Segre, N. Leyarovska, L. Chapman, W. Lavender, P. Plag, A. King, A. Kropf, B. Bunker, K. Kemner, P. Dutta, R. Duran, and J. Kaduk: 'The MRCAT insertion device beamline at the Advanced Photon Source ', Synchrotron Radiation Instrumentation, Stanford, CA, 1999, p. 419.
25. P. O'Day, M. Newville, P. Neuhoff, N. Sahai, and S. Carrol: 'X-Ray Absorption Spectroscopy of Strontium(II) Coordination I. Static and Thermal Disorder in Crystalline, Hydrated, and Precipitated Solids and in Aqueous Solution', *Journal of Colloid and Interface Science*, 222, (2000): p. 184.

26. B. Ravel and M. Newville: 'ATHENA, ARTEMIS, HEPHAESTUS: data analysis for X-ray absorption spectroscopy using IFEFFIT', *Journal of Synchrotron Radiation*, 12, (2005): p. 537.
27. A. A. Finch and N. Allison: 'Coordination of Sr and Mg in calcite and aragonite', *Mineralogical Magazine*, 71, 5 (2007): p. 539.
28. R. H. Parkman, J. M. Charnock, F. R. Livens, and D. J. Vaughan: 'A study of the interaction of strontium ions in aqueous solution with the surfaces of calcite and kaolinite', *Geochimica et Cosmochimica Acta*, 62, 9 (1998): p. 1481.
29. N. E. Pingitore Jr, F. W. Lytle, B. M. Davies, M. P. Eastman, P. G. Eller, and E. M. Larson: 'Mode of incorporation of Sr^{2+} in calcite: Determination by X-ray absorption spectroscopy', *Geochimica et Cosmochimica Acta*, 56, 4 (1992): p. 1531.
30. T. Shahwan, B. Zunbul, and D. Akar: 'Study of the scavenging behavior and structural changes accompanying the interaction of aqueous Pb^{2+} and Sr^{2+} ions with calcite', *Geochemical Journal*, 39, 4 (2005): p. 317.
31. S. A. Carroll, S. K. Roberts, L. J. Criscenti, and P. A. O'Day: 'Surface complexation model for strontium sorption to amorphous silica and goethite', *Geochemical Transactions*, 9, (2008): p. 1.
32. N. Sahai, S. A. Carroll, S. Roberts, and P. A. O'Day: 'X-ray absorption spectroscopy of strontium(II) coordination. II. Sorption and precipitation at kaolinite, amorphous silica, and goethite surfaces', *Journal of Colloid and Interface Science*, 222, 2 (2000): p. 198.
33. P. Chaurand, J. Rose, V. Briois, M. Salome, O. Proux, V. Nassif, L. Olivi, J. Susini, J. L. Hazemann, and J. Y. Bottero: 'New Methodological Approach for the Vanadium K-Edge X-ray Absorption Near-Edge Structure Interpretation: Application to the Speciation of Vanadium in Oxide Phases from Steel Slag', *Journal Physical Chemistry B*, 111, 19 (2007): p. 5101.
34. J. Wong, F. W. Lylte, R. P. Messmer, and D. H. Maylotte: 'K-edge absorption spectra of selected vanadium compounds', *Physical Review B*, 30, 10 (1984): p. 5596.
35. USEPA: 'Contaminant Information Sheets for the Final CCL 3 Chemicals', 214; 2009.